Fig.S1

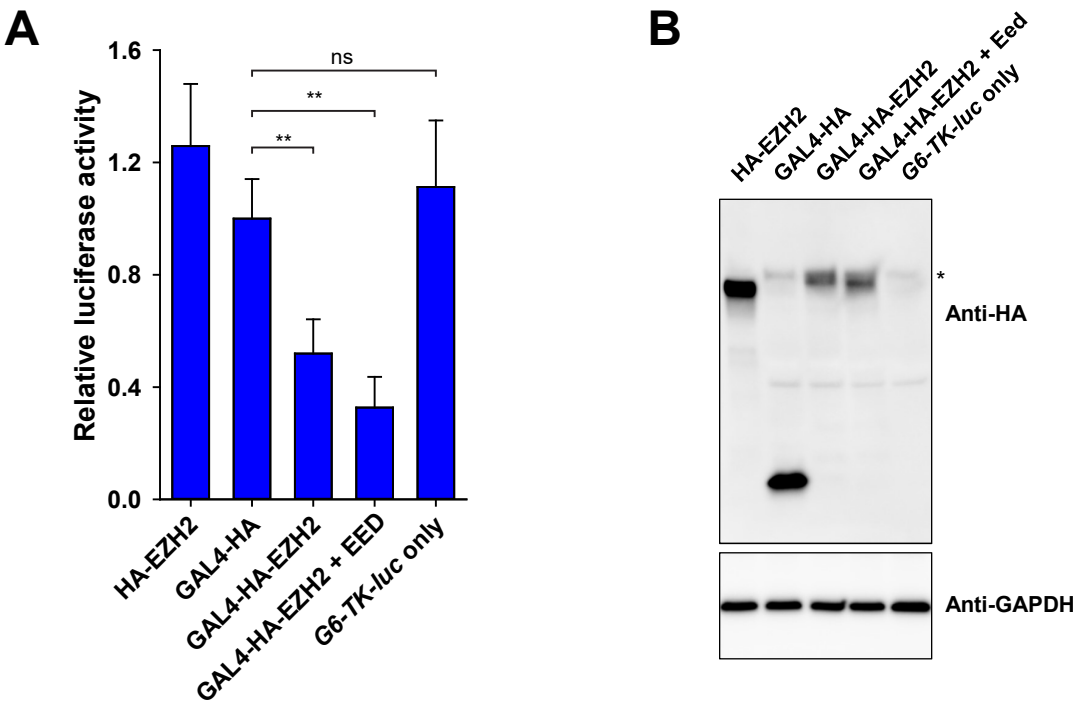

Fig. S1 EZH2-mediated reporter gene repression
(A) *G6-TK-luc* was used as the reporter plasmid. Reporter gene expression is shown relative to the 'GAL4-HA' empty vector control. 'HA-EZH2' lacks the GAL4DBD (GAL4 DNA-Binding Domain) tag for promoter targeting. **(B)** Protein expression level was checked by anti-HA antibody and anti-GAPDH served as the loading control.

Fig. S2

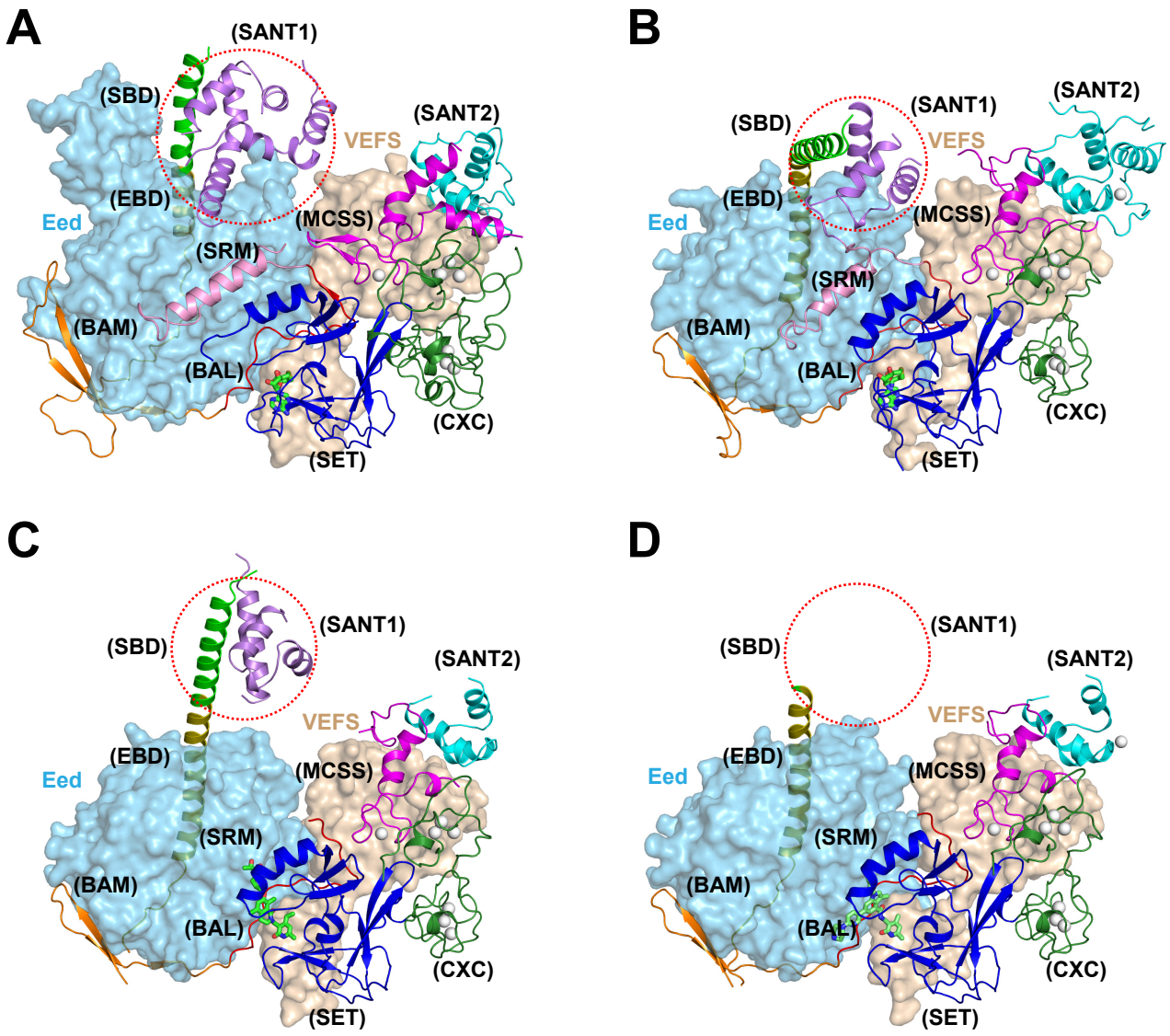

Fig. S2 Structural flexibility of the SBD−SRM−SANT1 module of EZH2 in PRC2
Crystal structures of (A) *ct*PRC2 PDB:5KJH, (B) *h*PRC2 PDB:5HYN, (C) *ac*PRC2 PDB:5IJ7, and (D) *h*PRC2 PDB:5WG6 are shown from the same view. EZH2 is shown in cartoon with its individual domains color-coded. EED and SUZ12(VEFS) are shown as blue and wheat surfaces, respectively. The EZH2(SBD) and EZH2(SANT1) are highlighted by a red dotted circle. The SBD−SRM−SANT1 module of EZH2 is partially or entirely disordered in some of the structures.

Fig. S3

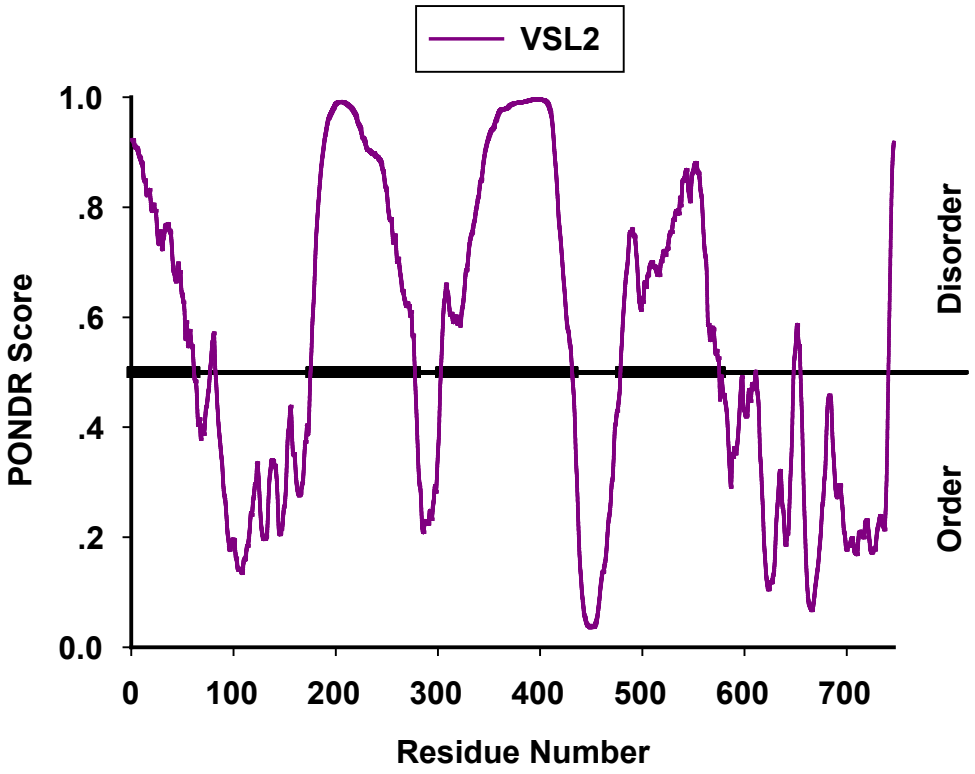

Fig. S3 The intrinsically disordered regions of EZH2
The intrinsically disordered regions of EZH2 are predicted using the VSL2 predictor in PONDR and highlighted by the black bars. One of the longest disordered regions of EZH2 largely overlaps with the EZH2(SANT1).

Fig. S4

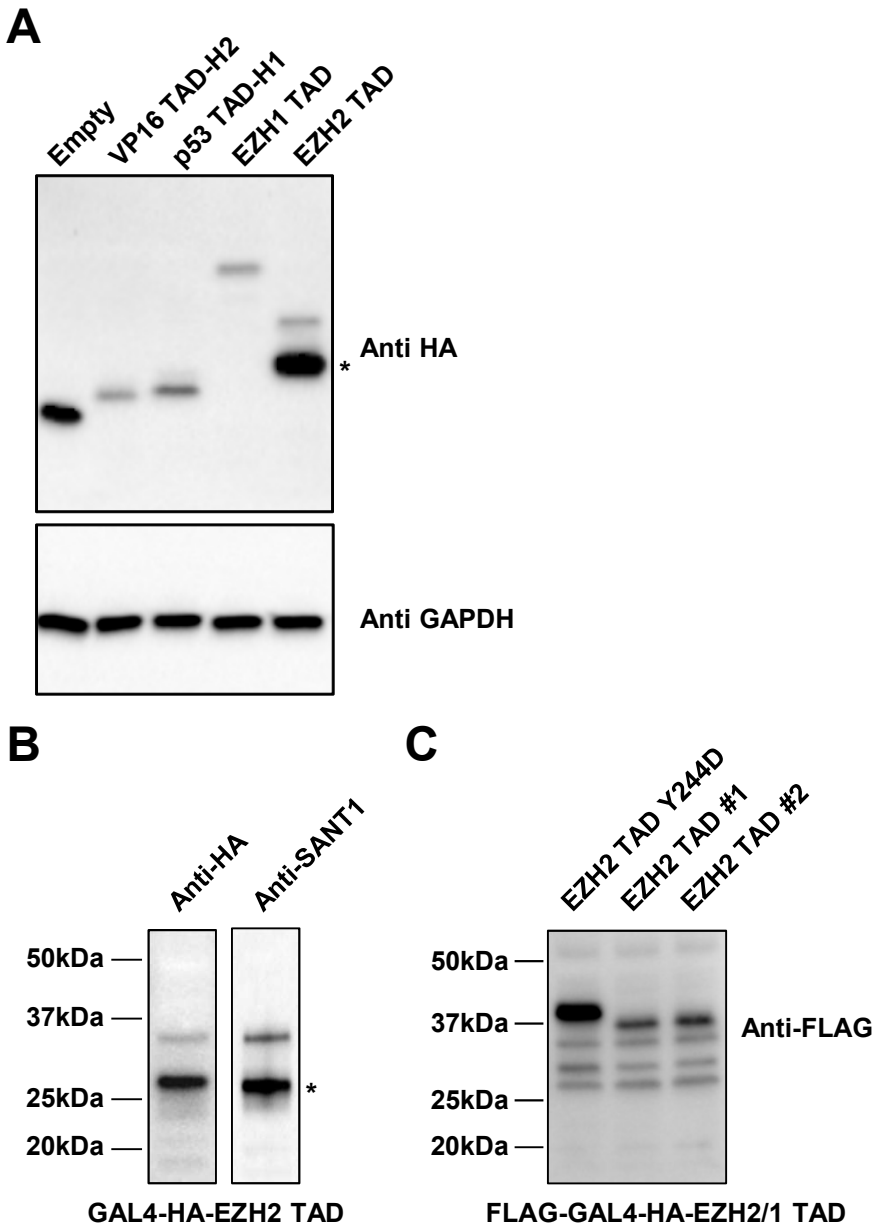

Fig. S4 Western blot of the expressed proteins in Fig. 1C

(A) Whole cell lysates of the luciferase reporter gene assay samples were detected by anti-HA antibody. Anti-GAPDH was used as the loading control. The strong band indicated by * represents a degradation product of the EZH2 TAD that does not contain the GAL4DBD tag. **(B)** and **(C)** Confirmation of the identity of the degradation band. In **(B)**, antibodies recognizing the HA tag (located in the middle of the construct) and the EZH2(SANT1) domain (located at the C-terminus of the construct) (BD Biosciences, Cat# 612666) both detected the full-length product (the band closer to the 37KDa protein standard) and the degradation product (the band closer to the 25KDa protein standard). In **(C)**, when a new N-terminal FLAG tag was added to the construct, anti-FLAG antibody detected the full-length band but not the strong degradation band that lacked the N-terminal FLAG-GAL4DBD tag. Representative constructs were checked in this way, including FLAG-GAL4DBD-HA-EZH2 TAD(Y244D) and FLAG-GAL4DBD-HA-EZH2 TAD ('#1' and '#2' indicate two independent clones of this construct).

Fig. S5

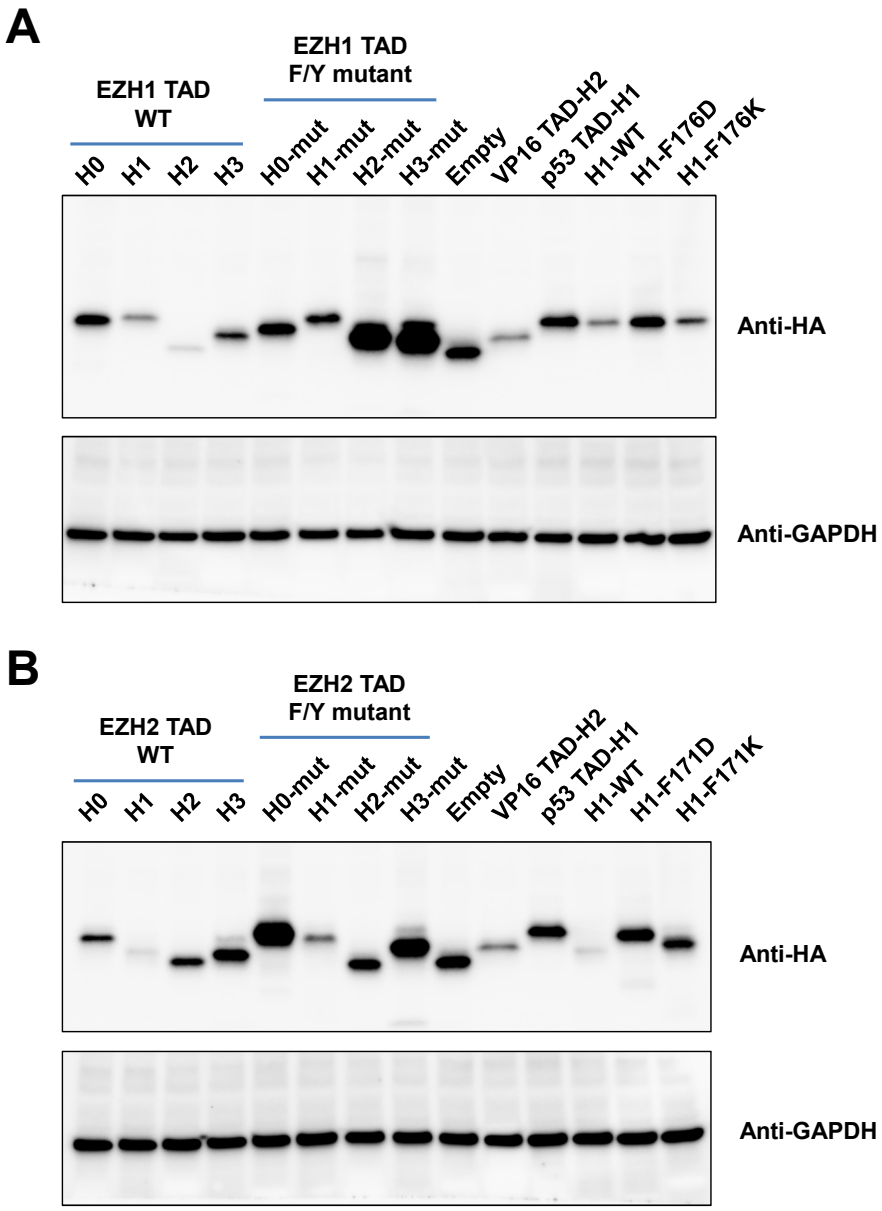

Fig. S5 Western blot of the expressed proteins in Fig. 1D and 1E
Whole cell lysates of the luciferase reporter gene assay samples were detected by anti-HA antibody. Anti-GAPDH was used as the loading control. **(A)** corresponds to **Fig. 1D** and **(B)** corresponds to **Fig. 1E.**

Fig. S6

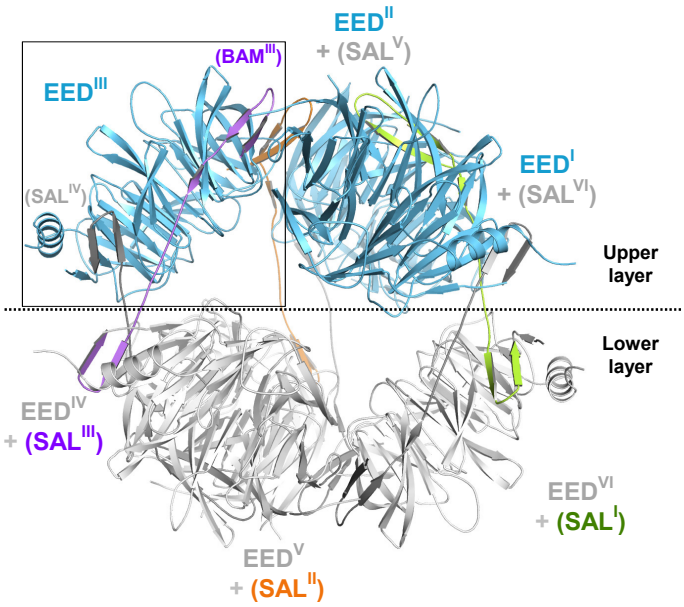

Fig. S6 Side view of the crystal structure of the EZH2−EED complex
Only the BAM and SAL domains of all six EZH2 molecules are shown with all other domains hidden. Identity of individual monomers is indicated by superscripts.

Fig. S7

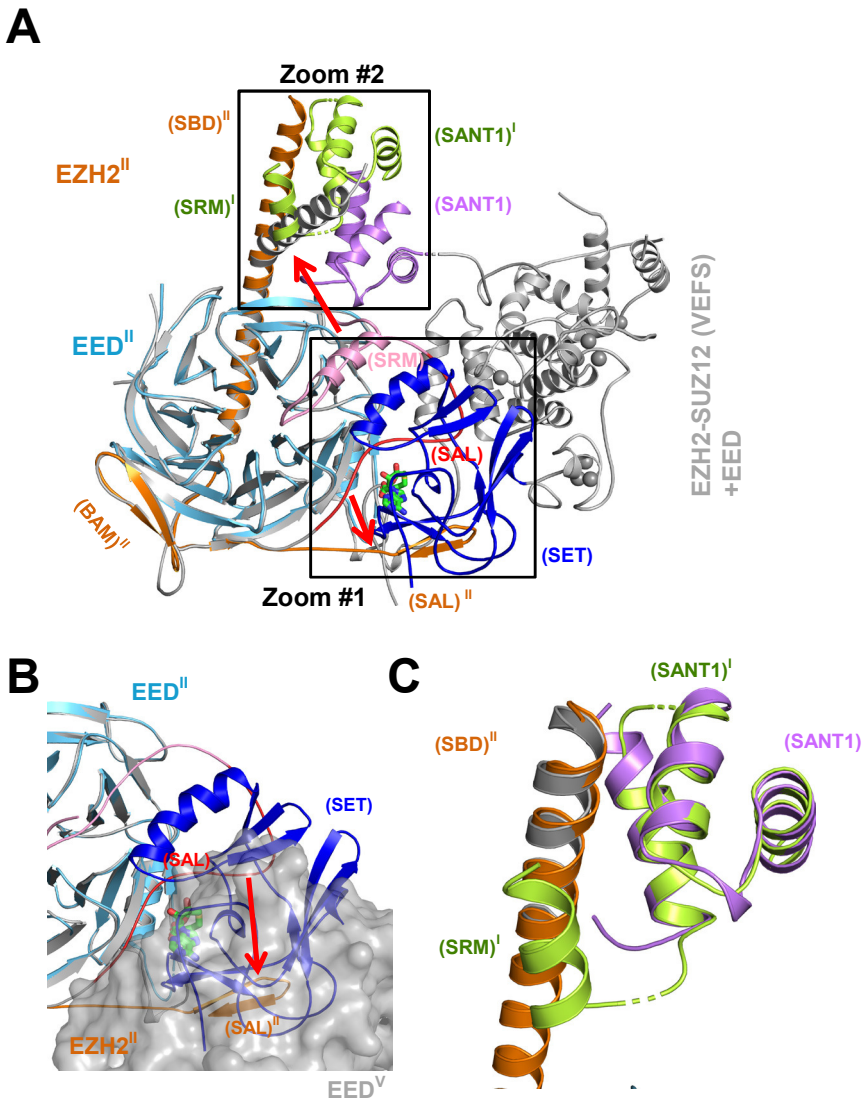

Fig. S7 Comparison of the current EZH2−EED structure to PRC2
(A) The current structure of EZH2−EED is aligned to the structure of human PRC2 (PDB:5HYN). The SAL and SRM−SANT1 regions are highlighted in black boxes. Red arrows represent the movement the indicated structural domains (SAL and SRM) from PRC2 to the current structure. **(B)** Zoom-in view of the SAL region. **(C)** Zoom-in view of the SRM−SANT1 region. The SBD was misaligned between the two structures in **(A)**, and the SBD−SRM−SANT1 modules from the two structures were re-aligned to each other in **(C)**.

Fig. S8

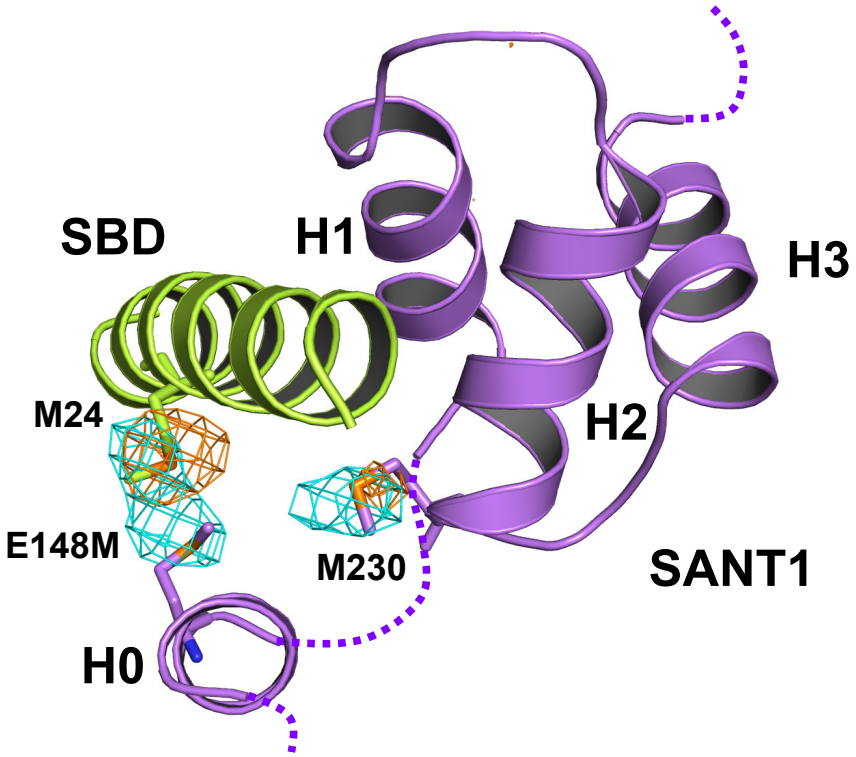

Fig. S8 Confirmation of the identity of helix H0 in the current structure of the EZH2−EED complex by anomalous signals

Cartoon representation of the EZH2^{III} TAD (magenta) and the EZH2^{I} SBD (limon) is shown to illustrate an E148M single mutation on helix H0. View is rotated from **Fig. 2C** along y-axis by 35°. E148 M on helix H0 together with two other methionine residues, M24 and M230, within the SBD−TAD helix bundle is shown in sticks. Anomalous signal from Se-SAD data is shown as orange meshes for WT EZH2−EED complex and cyan meshes for the E148M mutant.

Fig.S9

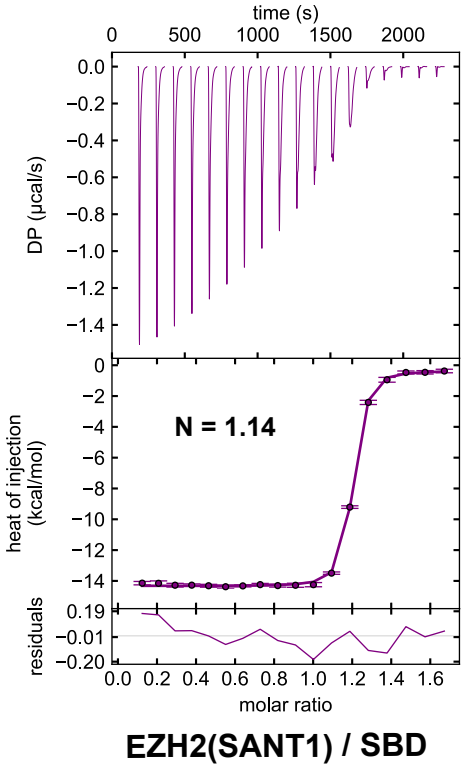

Fig. S9 ITC result of WT EZH2(SBD) WT binding to the WT EZH2(SANT1)
'N' represents the fitted stoichiometry of the binding. Kd value is reported in **Fig. 3A.**

Fig.S10

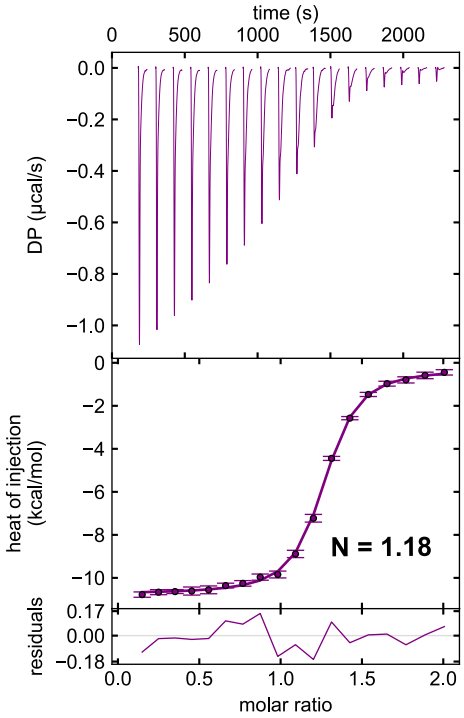

EZH2(SANT1)(Δ183-219) / EZH2(SBD)

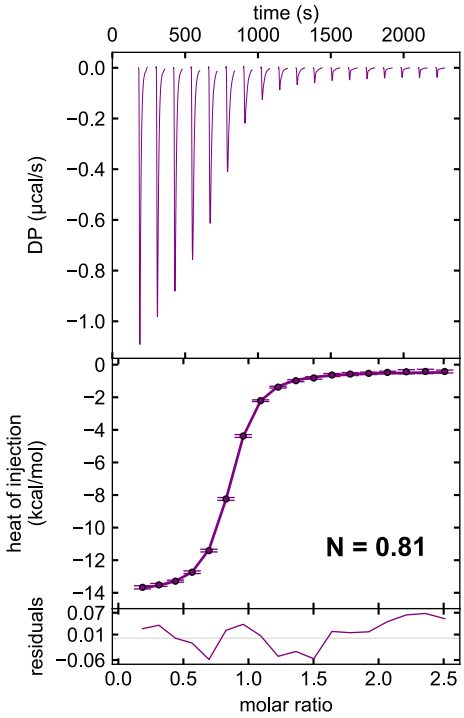

EZH2(SANT1)(Δ183-192) / EZH2(SBD)

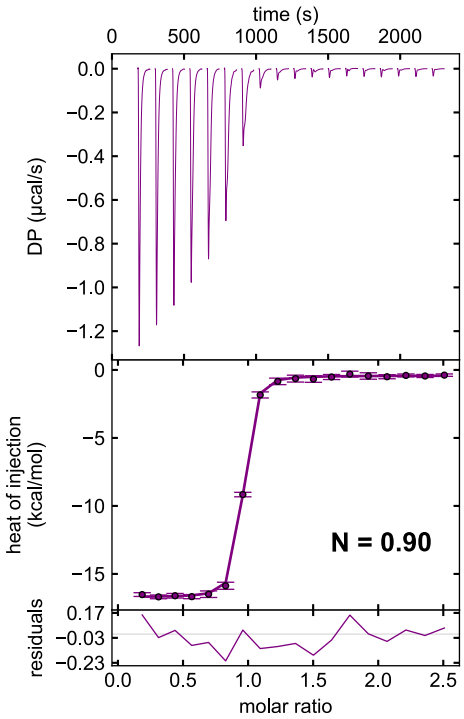

EZH2(SANT1)(Δ193-202) / EZH2(SBD)

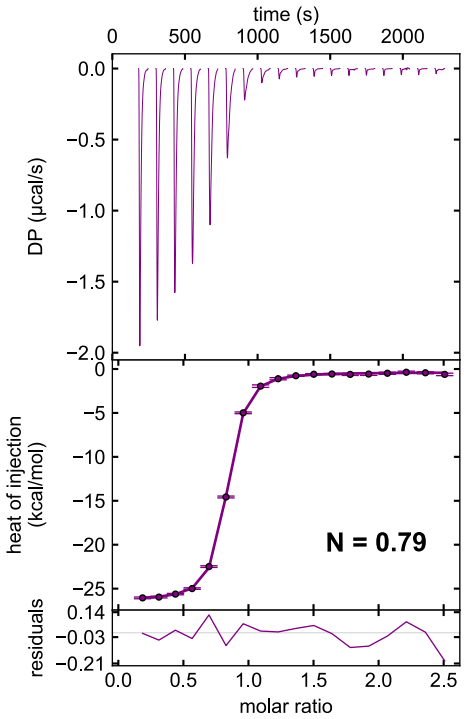

EZH2(SANT1)(Δ203-219) / EZH2(SBD)

Fig.S10 ITC results of WT EZH2(SBD) binding to the truncated variants of EZH2(SANT1) The linker region between the helices H1 and H2 of EZH 2 TAD was replaced with a flexible linker as follows: (1) residues 183-219 were replaced by a GSSG linker, (2) residues 183-192 were replaced by a $(GGS)_3G$ linker, (3) residues 193-202 were replaced by a $(GGS)_3G$ linker, and (4) residues 203-219 were replaced by a $(GGS)_5GG$ linker. 'N' represents the fitted stoichiometry of the binding. Kd values are reported in **Fig. 3A.**

Fig.S11

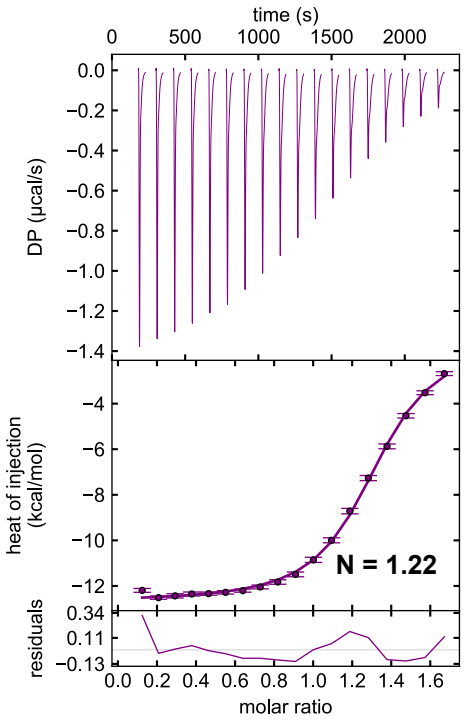

EZH2(SANT1) / EZH2(SBD)-S21p

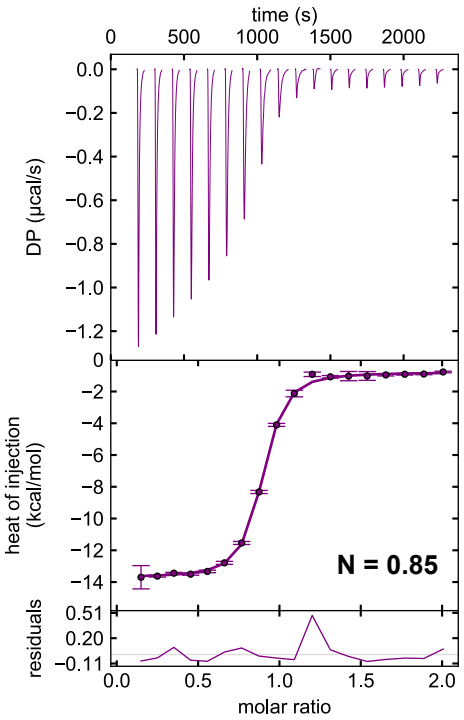

EZH2(SANT1) / EZH2(SBD)-S21D

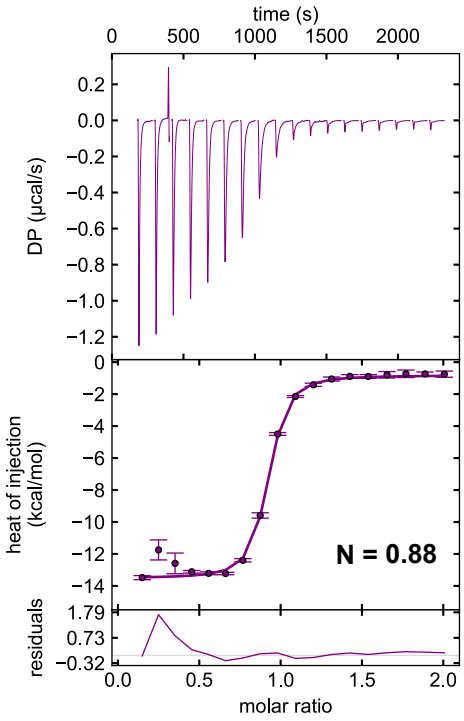

EZH2(SANT1) / EZH2(SBD)-S21E

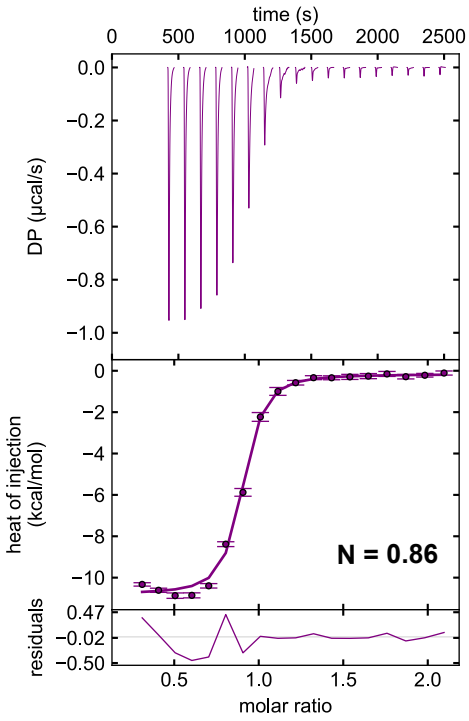

EZH2(SANT1) / EZH2(SBD)-S21A

Fig. S11 ITC results of WT EZH2(SANT1) binding to the EZH2(SBD)-S21p, -S21D, -S21E and -S21A peptides

'N' represents the fitted stoichiometry of the binding. Kd value is reported in **Fig. 3A.**

Fig.S12

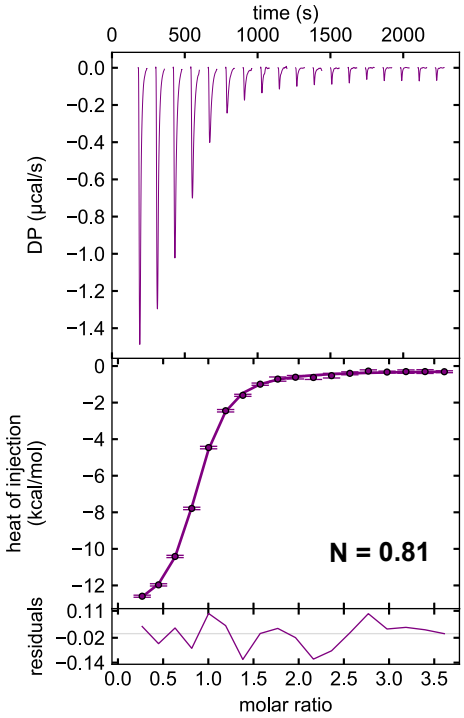

Fig. S12 ITC result of WT EZH1(SBD) binding to the EZH1(SANT1)
'N' represents the fitted stoichiometry of the binding. Kd value is reported in **Fig. 3A.**

Fig.S13

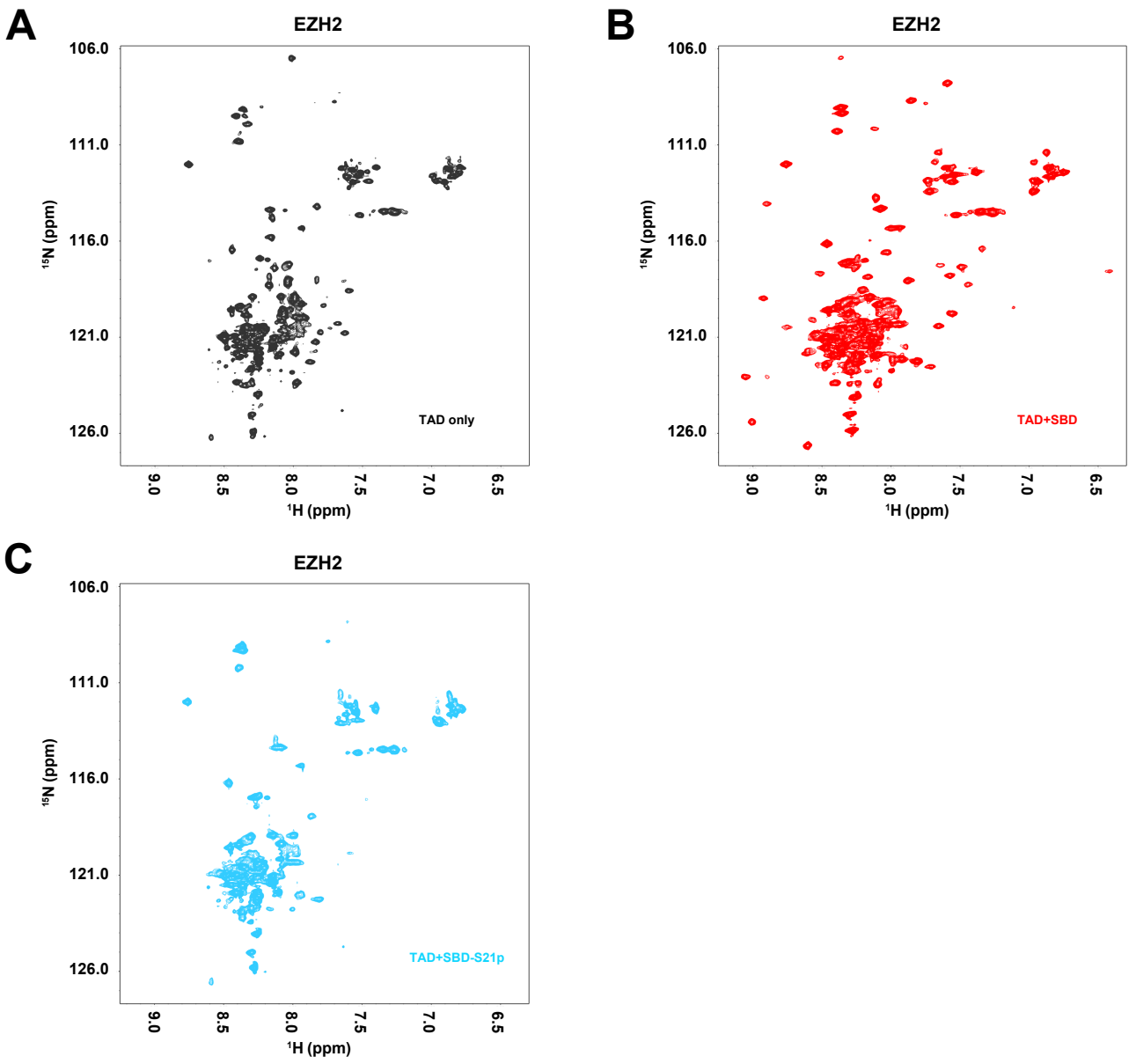

Fig. S13 ^{1}H-^{15}N HSQC spectra of the ^{15}N-labeled EZH2 TAD, TAD+SBD and TAD+SBD-S21p
^{1}H-^{15}N HSQC spectra of ^{15}N-labeled EZH2 TAD were collected at ~50μM in the absence or presence of 1.2X synthesized SBD peptide (~60uM). Individual spectrum of **(A)** TAD alone in black, **(B)** TAD+SBD in red and **(C)** TAD+SBD-S21p in cyan are shown.

Fig.S14

A

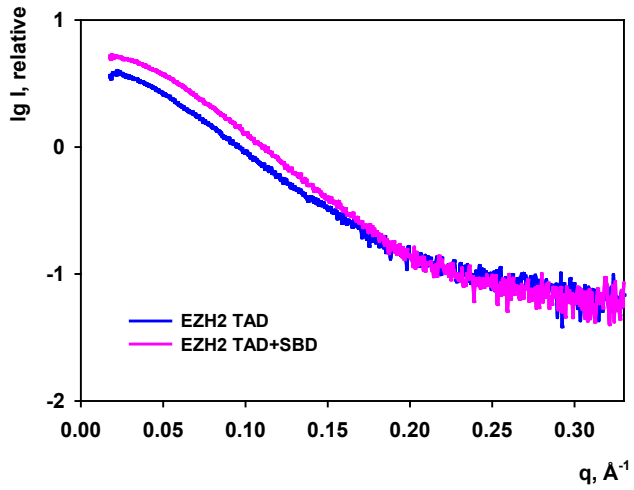

B

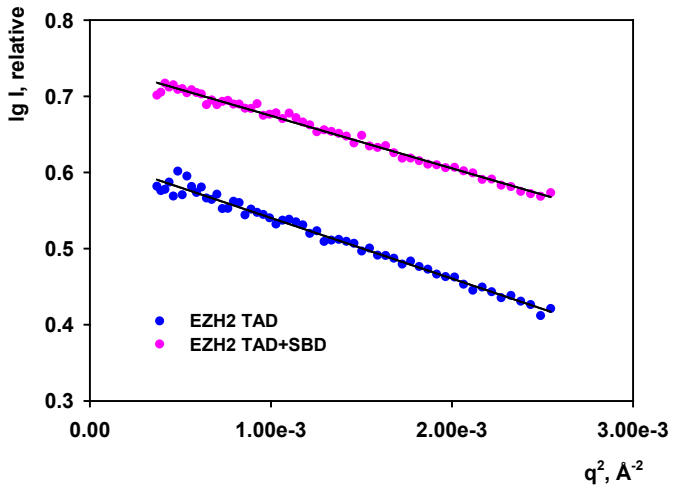

C

Protein sample	R_g (Å)	I (0)
EZH2 TAD	23.49±0.31	4.18±0.013
EZH2 TAD+SBD	22.00±0.70	5.56±0.011

Fig. S14 SAXS analysis of the EZH2 TAD in the unbound and SBD-bound states
(A) Scattering profiles of the unbound EZH2 TAD (blue) and the SBD-bound EZH2 TAD (purple) were generated by averaging 33 successive 0.3 s exposures. The plots are shown as log[I(q)] versus q. **(B)** Guinier plots were shown as lg[I(q)] vs q^2. The wide q range linearity suggests that neither inter-molecular interactions nor aggregation was observed during data collection. **(C)** Values of R_g (radius of gyration) and I(0) (Intensity at q=0) were analyzed in PRIMUS by Guinier plot approximation.

Fig. S15

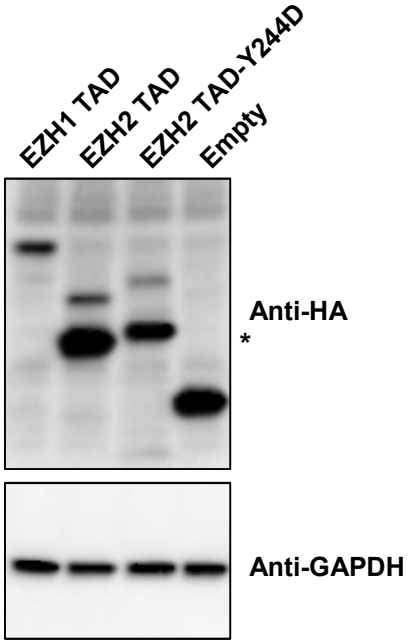

Fig. S15 Western blot of the expressed proteins in Fig. 3G
Whole cell lysates of the luciferase reporter gene assay samples were detected by anti-HA antibody. Anti-GAPDH was used as the loading control. The strong bands indicated by * represent a degradation product of the EZH2 TAD that does not contain the GAL4DBD tag.

Fig. S16

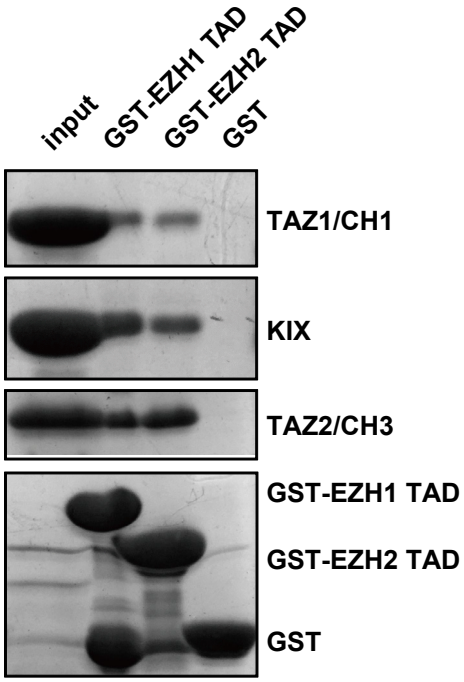

Fig. S16 *In vitro* GST pull-down of selected p300 domains by the TADs of EZH1 and EZH2
Input for the prey p300 domains are shown. GST-EZH1 TAD and GST-EZH2-TAD served as the bait and GST was used as the negative control.

Fig. S17

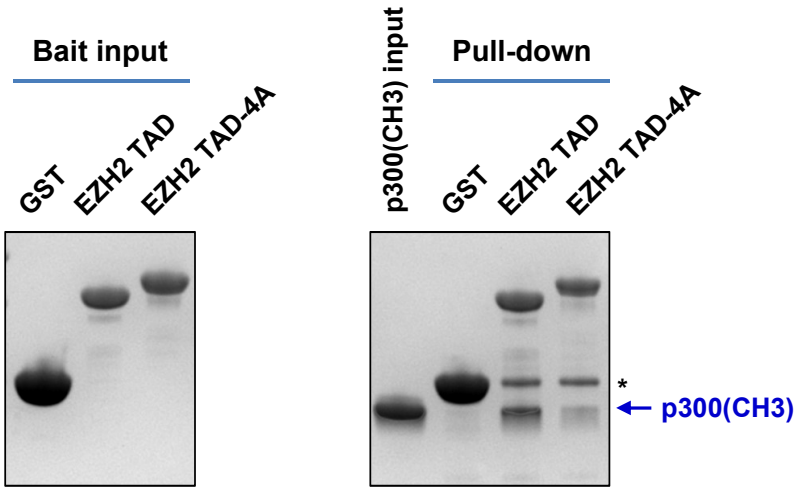

Fig. S17 *In vitro* GST pull-down of the p300(CH3) with the EZH2 TAD and the EZH2-TAD-4A mutant

The binding of the p300(CH3) to the WT EZH2-TAD and the EZH2-TAD-4A mutant was compared. The bait input (GST, GST-EZH2 TAD and GST-EZH2 TAD-4A) is shown in the left panel and the prey input (p300(CH3)) is shown in the right panel. The band indicated by * represents GST.

Fig.S18

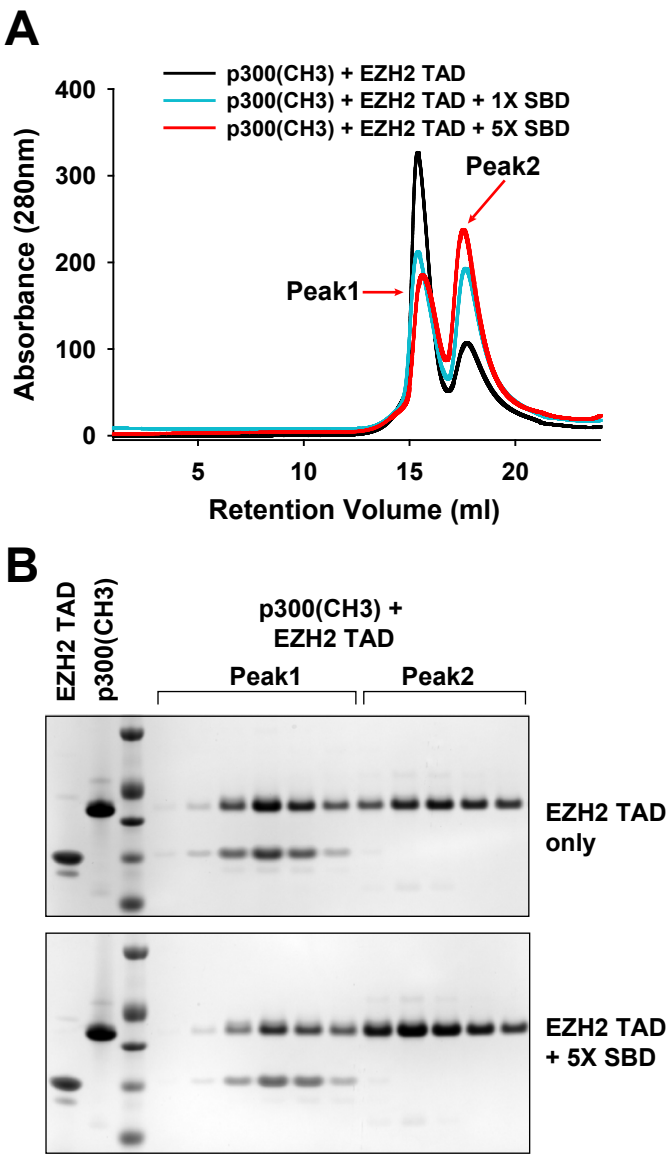

Fig. S18 Disruption of the stoichiometric complex between the EZH2 TAD and the p300(CH3) by the SBD of EZH2

Protein/peptide mixtures were loaded to the SEC column in three runs, containing (1) TAD + 1.5×CH3, (2) TAD + 1.5×CH3 + 1×SBD and (3) TAD + 1.5×CH3 + 5×SBD. SDS-PAGE gels for the cases (1) and (3) are shown. Peaks 1 and 2 represent the EZH2 TAD-p300(CH3) binary complex and the excessive unbound p300(CH3), respectively.

Fig.S19

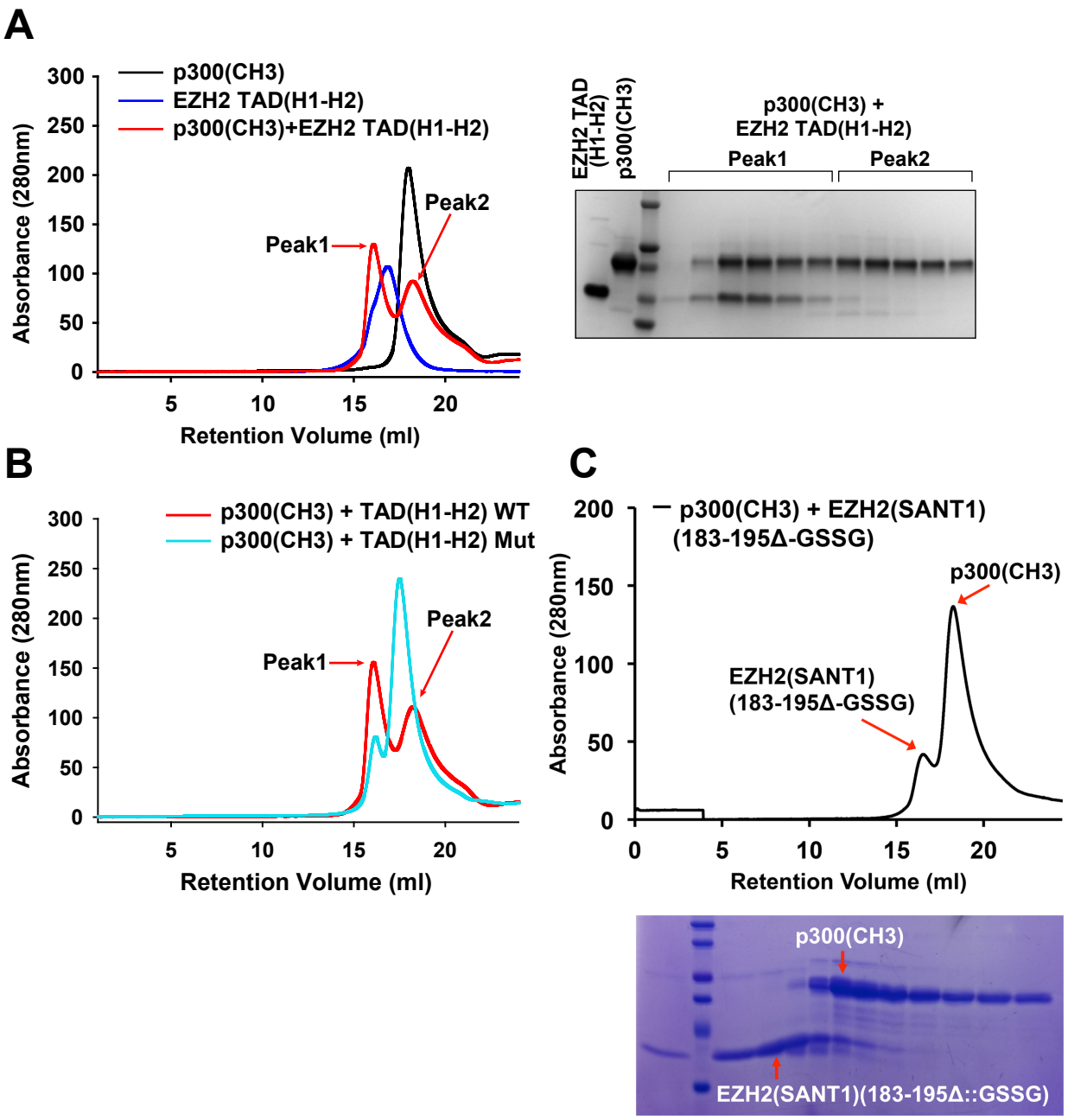

Fig. S19 Complex formation between p300 (CH3) and the EZH2 TAD (H1-H2) or EZH2(SANT1)

(A) The SEC elution profile for the WT EZH2 TAD (H1-H2) bound to the p300(CH3) is shown. The profiles of the individual subunits of the binary complex are shown for comparison. SDS-PAGE gel for the co-eluted EZH2 TAD(H1-H2)-p300(CH3) complex is provided. Peaks 1 and 2 represent the EZH2 TAD-p300(CH3) binary complex and the excessive unbound p300(CH3), respectively. **(B)** The SEC elution profiles of the WT binary complex and the mutant binary complex harboring the F171A/F224A double mutation ('EZH2-TAD-2A') are compared. **(C)** The SEC elution profile of p300(CH3) bound to a variant of EZH2(SANT1) (residues 159-254) with residues 183-219 replaced by a "GSSG" sequence.

Fig. S20

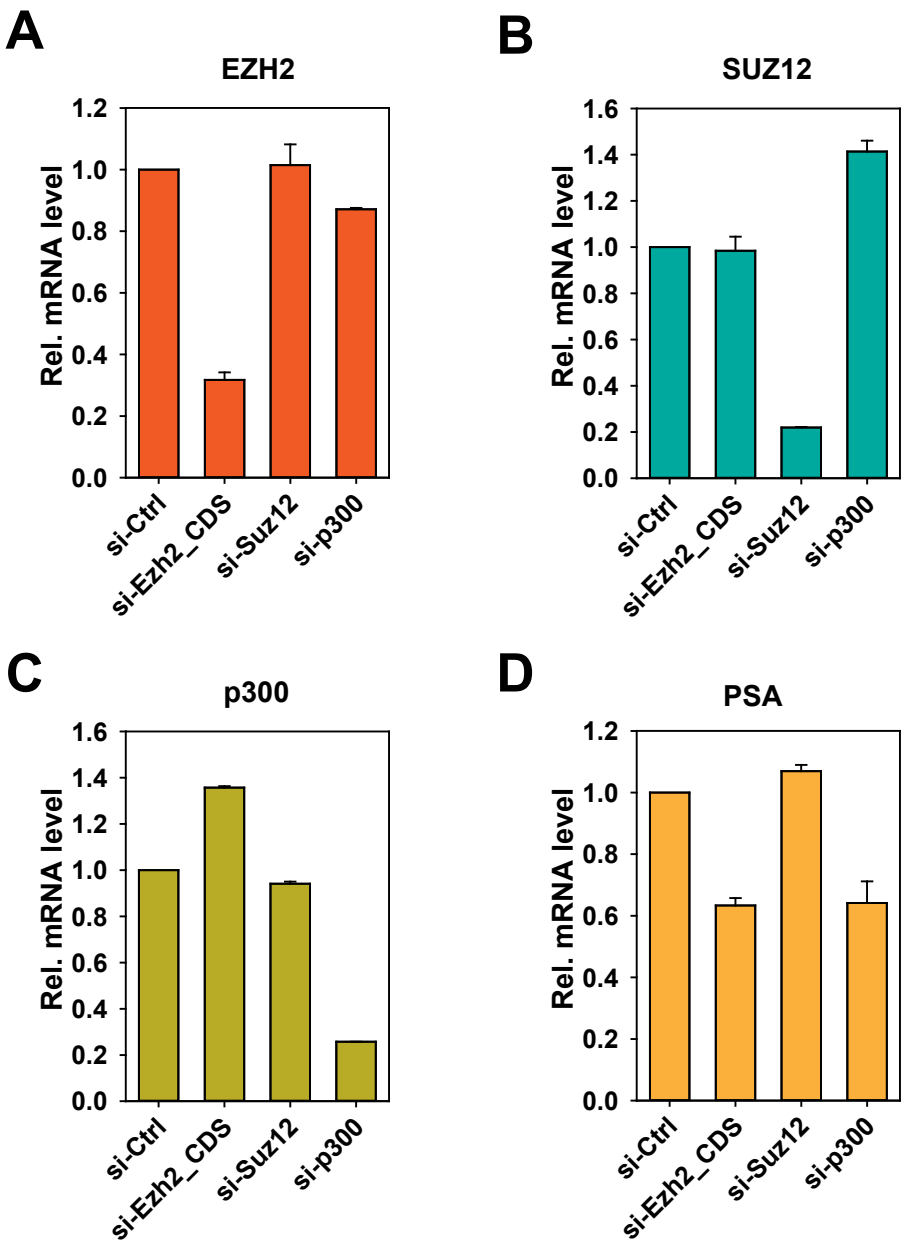

Fig. S20 PSA gene expression analysis in siRNA-treated LNCaP cells
LNCaP cells were transfected with either control siRNA (si-Ctrl) or siRNAs targeting EZH2 (si-EZH2_CDS), SUZ12 (si-SUZ12) or p300 (si-p300). Total RNAs were isolated and real-time RT-PCR was performed 48 hours post transfection. Relative mRNA levels were shown from three independent replicates using GAPDH as the internal control. The knockdown efficiency and specificity were assessed by RT-PCR in panels **(A)**, **(B)** and **(C)**. In panel **(D)**, knockdown of EZH2 and p300 but not SUZ12 hampered PSA gene expression.

Fig. S21

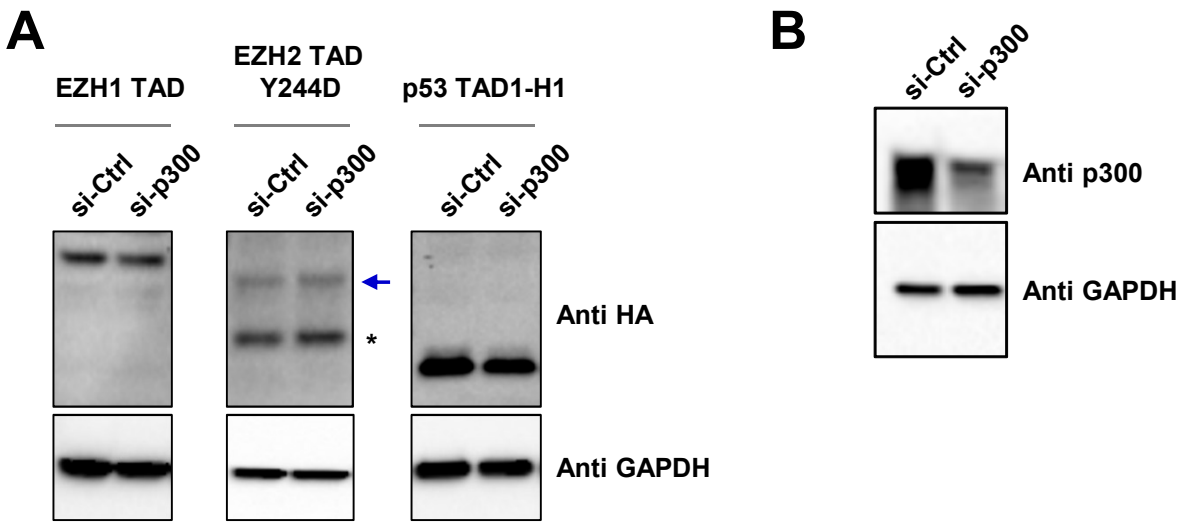

Fig. S21 Western blot of the protein expression in Fig. 5A
(A) Whole cell lysates of the luciferase reporter gene assay samples were detected by anti-HA antibody. Degradation bands are marked by *. **(B)** Si-p300 mediated knockdown efficiency was confirmed by anti-p300 antibody. GAPDH was used as the loading control.

Fig. S22

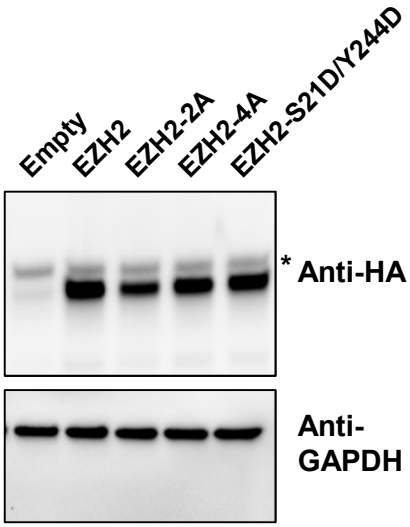

Fig. S22 Western blot of the expressed proteins in Fig. 5B
Whole cell lysates of the luciferase reporter gene assay samples were detected by anti-HA antibody. GAPDH was used as the loading control. Non-specific Western signal was indicated by *.

Fig.S23

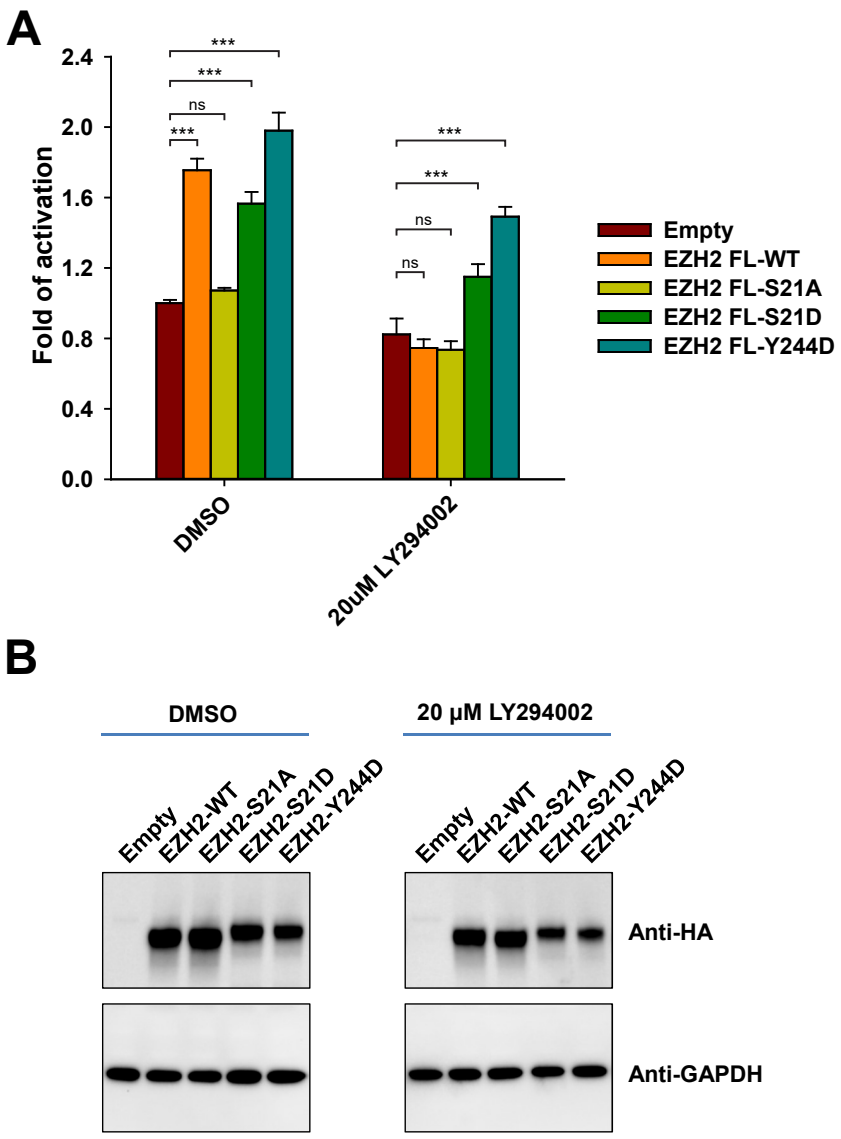

Fig. S23 AR promoter-based reporter gene activation assay in 22Rv1 cells in the absence and presence of a kinase inhibitor

(A) Fold of reporter gene activation is shown relative to pCS2+ empty vector. 22Rv1 cells were pretreated with either DMSO vehicle or 20μM LY294002. Gene activation of HA-tagged EZH2-FL-WT and EZH2-FL-S21/Y244 mutants were examined. **(B)** Western blot of the expressed HA tagged EZH2 WT/mut in **(A)** . GAPDH was used as the loading control.

Fig. S24

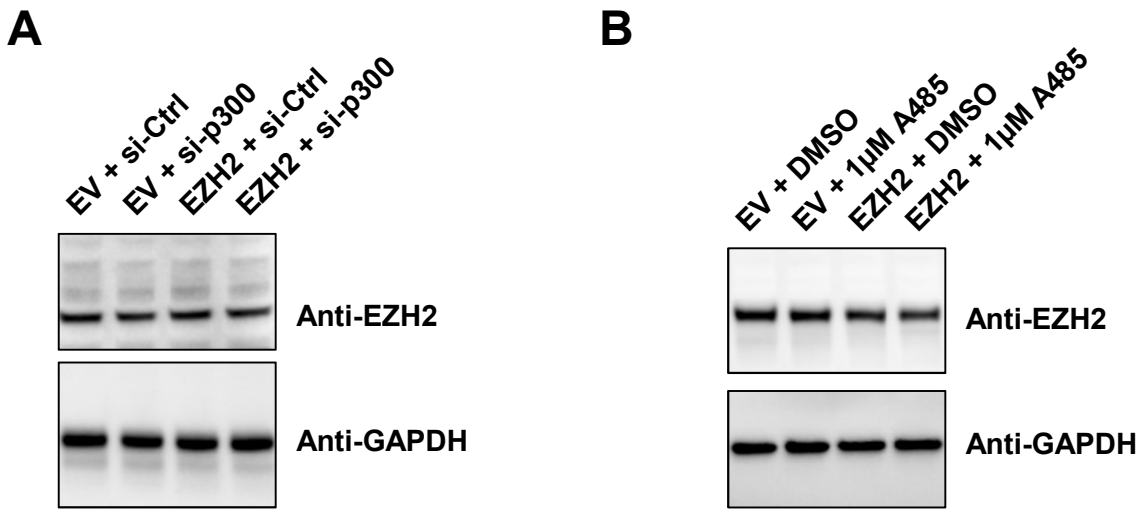

Fig. S24 Western blot of the expressed proteins in Fig. 5C and 5D
(A) corresponds to **Fig. 5C** and **(B)** corresponds to **Fig. 5D**. Whole cell lysates of the luciferase reporter gene assay samples were detected by anti-HA antibody. GAPDH was used as the loading control.

Table S1. Data collection and refinement statistics.

Crystal	EZH2-EED
Diffraction data	
Wavelength (Å)	0.97946
Space group	$P222_1$
a, b, c (Å)	181.6, 114.7, 113.5
α, β, γ (°)	90.0, 90.0, 90.0
Resolution range (Å)	50.00 - 2.90 (2.95 - 2.90)
R_{sym} or R_{merge}	0.120 (1.329)
Mean I/σ (I)	15.1 (1.0)
R_{pim} (%)	5.2 (57.9)
$CC_{1/2}$ (%)	99.4 (56.1)
Completeness (%)	99.8 (97.3)
Redundancy	13.7 (9.8)
Refinement	
Bumber of reflections	54453
R_{work}/R_{free}	0.19/0.22
Number of non-hydrogen atoms	12736
EZH2	4016
EED	8720
Protein residues	1562
Average B-factor (Å^2)	59.80
EZH2	78.68
EED	51.14
R.m.s deviations	
Bond lengths (Å)	0.008
Bond angles (º)	0.99
Ramachandran	
Favored (%)	96.85
Allowed (%)	3.15
Outliers (%)	0.00

Statistics for the highest-resolution shell are shown in parentheses.

Table S2. Detailed information of target gene in luciferase reporter assay

Luciferase Assay	Vector Diagrams	Name	Gene Fragment
Gal4-based	(pCS2+)-GAL4DBD-HA +**Gene Fragment**	Empty	none
		EZH2 FL	EZH2 (1-746)
		EZH2 TAD	EZH2 (135-254)
		EZH2 TAD Y244D	EZH2 (135-254) Y244D
		EZH1 TAD	EZH1 (136-267)
		VP16 TAD-H2	VP16 (469-487)
		p53 TAD-H1	p53 (9-27)
		EZH1 TAD-H0	EZH1 (136-160)
		EZH1 TAD-H0 mutant	EZH1 (136-160) F146A
		EZH1 TAD-H1	EZH1 (161-187)
		EZH1 TAD-H1 mutant	EZH1 (161-187) F176A
		EZH1 TAD-H1 F176D	EZH1 (161-187) F176D
		EZH1 TAD-H1 F176K	EZH1 (161-187) F176K
		EZH1 TAD-H2	EZH1 (233-247)
		EZH1 TAD-H2 mutant	EZH1 (233-247) F237A
		EZH1 TAD-H3	EZH1 (248-267)
		EZH1 TAD-H3 mutant	EZH1 (248-267) Y257A
		EZH2 TAD-H0	EZH2 (135-158)
		EZH2 TAD-H0 mutant	EZH2 (135-158) F145A
		EZH2 TAD-H1	EZH2 (159-182)
		EZH2 TAD-H1 mutant	EZH2 (159-182) F171A
		EZH2 TAD-H1 F171D	EZH2 (159-182) F171D
		EZH2 TAD-H1 F171K	EZH2 (159-182) F171K
		EZH2 TAD-H2	EZH2 (220-234)
		EZH2 TAD-H2 mutant	EZH2 (220-234) F224A
		EZH2 TAD-H3	EZH2 (235-254)
		EZH2 TAD-H3 mutant	EZH2 (235-254) Y244A
AR promoter driven	(pCS2+) + **Gene Fragment**	Empty	HA
		EZH2 FL	HA-EZH2 (1-746)
		EZH2 FL-2A	HA-EZH2 (1-746) F171A/F224A
		EZH2 FL-4A	HA-EZH2 (1-746) F145A/F171A/F224A/Y244A
		EZH2 FL-S21D/Y244D	HA-EZH2 (1-746) S21D/Y244D

Table S3. Oligonucleotide sequences that were used in this study

Name	**Sequence**	Application
si-EZH2 (CDS)	AAGAGGUUCAGACGAGCTGAU[dT][dT]	Knockdown
si-SUZ12	CUGUUACCAAGCUCCGUGA[dT][dT]	Knockdown
si-p300	GGACUACCCUAUCAAGUAA[dT][dT]	Knockdown
GAPDH-F	TGCACCACCAACTGCTTAGC	RT-PCR
GAPDH-R	GGCATGGACTGTGGTCATGAG	RT-PCR
EZH2-F	TTGTTGGCGGAAGCGTGTAAAATC	RT-PCR
EZH2-R	TCCCTAGTCCCGCGCAATGAGC	RT-PCR
SUZ12-F	AAACGAAATCGTGAGGATGG	RT-PCR
SUZ12-R	CCATTTCCTGCATGGCTACT	RT-PCR
p300-F	AACAGCAGCTCAACCATCCA	RT-PCR
p300-R	TCCGGCGTAGGAAATATGGC	RT-PCR
PSA-F	ACGCTGGACAGGGGGCAAAAG	RT-PCR
PSA-R	GGGCAGGGCACATGGTTCACT	RT-PCR